APPLIED ORGANOMETALLIC CHEMISTRY
Appl. Organometal. Chem. 2003; **17**: 52–62
Published online in Wiley InterScience (www.interscience.wiley.com). DOI:10.1002/aoc.380

tert-Butoxysilanols as model compounds for labile key intermediates of the sol–gel process: crystal and molecular structures of $(t\text{-BuO})_3SiOH$ and $HO[(t\text{-BuO})_2SiO]_2H$†

Jens Beckmann[1]*, Dainis Dakternieks[1], Andrew Duthie[1], Megan L. Larchin[1] and Edward R. T. Tiekink[2]‡

[1]Centre for Chiral and Molecular Technologies, Deakin University, Geelong, Vic. 3217, Australia
[2]Department of Chemistry, The University of Adelaide, Adelaide, SA 5005, Australia

Received 19 June 2002; Revised 26 July 2002; Accepted 6 August 2002

The *tert*-butoxychlorosilanes $(t\text{-BuO})_3SiCl$ (1), $(t\text{-BuO})_2SiCl_2$ (2), and $[(t\text{-BuO})_2SiCl]_2O$ (3) were prepared by the reaction of $SiCl_4$ or $(Cl_3Si)_2O$ with *t*-BuOK. Subsequent hydrolysis afforded the *tert*-butoxysilanols $(t\text{-BuO})_3SiOH$ (4), $(t\text{-BuO})_2Si(OH)_2$ (5), $HO[(t\text{-BuO})_2SiO]_2H$ (6) in high yields. The controlled condensation of 2 and 5 provided $HO[(t\text{-BuO})_2SiO]_3H$ (7) in reasonable yields. The tendency of 4–7 to undergo self-condensation is small, thus enabling their characterization in solution and in the solid state by ^{29}Si NMR spectroscopy, IR spectroscopy and electrospray mass spectrometry, and in the case of 4 and 6 also by X-ray diffraction. The key feature of the crystal structures is the incorporation of *tert*-butoxy groups into the hydrogen bonding. The results obtained are discussed in relation to the sol–gel process. Copyright © 2002 John Wiley & Sons, Ltd.

KEYWORDS: Sol–gel process; silicon; hydrogen bonds; X-ray diffraction; NMR spectroscopy

INTRODUCTION

The sol–gel process constitutes the most versatile and powerful method for the low-temperature preparation of a vast variety of amorphous metal oxide materials, such as films, fibres, ceramics, and glasses.[1–3] It involves the partial hydrolysis of metal alkoxides, $M(OR)_n$ (M = transition or main group metal; R = alkyl or aryl), to produce intermediate species containing hydroxy groups, followed by condensation of the hydroxy groups and residual alkoxy groups to form three-dimensional networks, and finally hydrated metal oxides. Once the process has been initiated, the hydrolysis and condensation occur simultaneously, albeit with different reaction rates that largely depend on the reaction conditions. The morphology and texture of the oxide materials can be widely influenced by processing parameters, such as concentration of the metal alkoxides, reaction temperature, solvent, amount of water, and catalyst used. All these parameters have some effect on the kinetics. Given the complex nature of the sol–gel process, studies on the intermediate species and their reaction pathways show promise in providing a deeper insight into the mechanisms involved.[4]

Considerable effort has been devoted towards the understanding of the sol–gel process of silicon alkoxides $Si(OR)_4$ (R = Me, Et, *n*-Pr) to produce hydrated silica, $[SiO_{n/2}(OH)_{4-n}]_m$.[5] In these systems, both the hydrolysis and condensation occur slowly enough to enable mechanistic studies of the process in great detail by methodologies such as ^{29}Si NMR, Raman and IR spectroscopy, trimethylsilylation/gas and liquid chromatography, and electrospray ionization mass spectrometry (ESI MS).[1–3] In particular, ^{29}Si NMR spectroscopy suggests the existence of discrete linear and cyclic alkoxy-silanols and -siloxanes with a reasonably long lifetime in the early stage of the process, such as $(RO)_3SiOH$ (**I**), $(RO)_3SiOSi(OR)_3$ (**II**), $(RO)_2Si(OH_2)$ (**III**), $HO[(RO)_2SiO]_nH$ (**IV**), and $[(RO)_2SiO]_n$ (**V**) (Scheme 1).[6–21] Further studies have shown that both hydrolysis and condensation rates of these intermediates decrease with the

*Correspondence to: J. Beckmann, Centre for Chiral and Molecular Technologies, Deakin University, Geelong, Vic. 3217, Australia.
E-mail: beckmann@deakin.edu.au
†Presented at the XXth International Conference on Organometallic Chemistry, 7–12 July 2002, Corfu, Greece.
‡Department of Chemistry, National University of Singapore, Singapore 117543, Singapore.
Contract/grant sponsor: Australian Research Council.

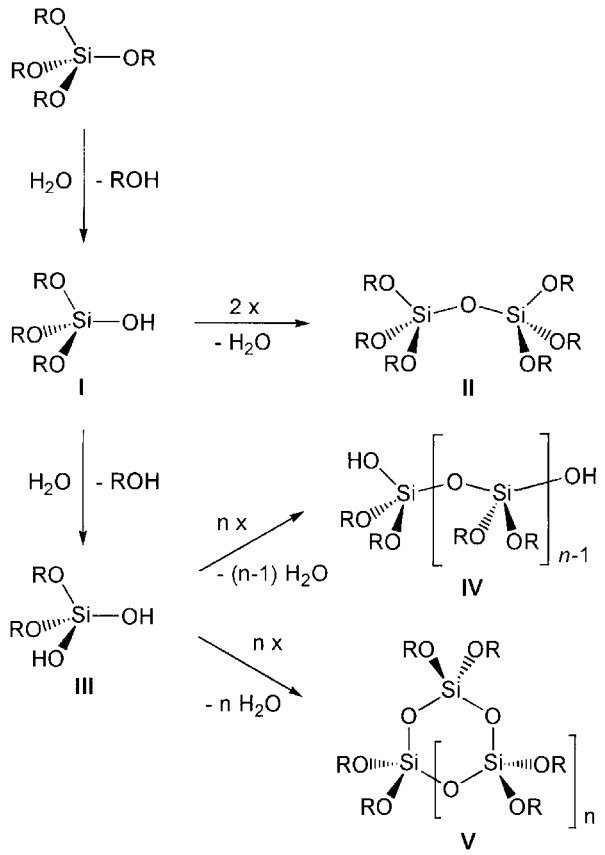

Scheme 1. Principle reaction pathway of the sol–gel process of alkoxysilanes (only the water-forming condensation is considered).

increasing number and bulkiness of the alkoxy groups.[22] Consequently, alkoxy-silanols and -siloxanes containing very large alkoxy groups might be sufficiently kinetically inert to allow their isolation. Their characterization would be useful for a comparison with their more labile counterparts of the sol–gel process. Indeed, a great number of stable alkoxy-silanols and -siloxanes has been described in previous works.[23–33] Surprisingly, these compounds still remain poorly characterized, particularly when considering state-of-the-art methodologies such as ^{29}Si NMR spectroscopy and X-ray crystallography. Additionally, their relevance for the sol–gel process has not yet been put forward. However, two fully characterized exceptions, namely $[(t\text{-BuO})_3\text{SiOSi(OH)}_2]_2\text{O}$ and $(\text{RO})_3\text{SiOH}$ (RO = (1*S*)-*endo*-(−)-bornoxy), have been published only recently.[34,35] The key feature of both structures is the involvement of alkoxy groups in hydrogen bonding.

The *tert*-butoxysilanols $(t\text{-BuO})_3\text{SiOH}$ and $(t\text{-BuO})_2\text{Si(OH)}_2$ have been frequently utilized for the synthesis of metallasiloxanes, which represent excellent single-source precursors for the mild conversion into atomically well-mixed metal oxide/silica materials.[36–45] This concept has not yet been extended to incorporate potentially chelating 1,1,3,3-tetraalkoxy-1,3-disiloxan-1,3-diols, or 1,1,3,3,5,5-hexaalkoxy-1,3,5-trisiloxan-1,5-diols, such as $\text{HO}[(t\text{-BuO})_2\text{SiO}]_2\text{H}$ and $\text{HO}[(t\text{-BuO})_2\text{SiO}]_3\text{H}$, which might give single-source precursors with different properties.[46–49] The same silanols also hold potential as protecting groups in organic synthesis.[50–52]

In the present study, we report the improved synthesis of a series of *tert*-butoxysilanols, $(t\text{-BuO})_3\text{SiOH}$, $(t\text{-BuO})_2\text{Si(OH)}_2$, $\text{HO}[(t\text{-BuO})_2\text{SiO}]_2\text{H}$, and $\text{HO}[(t\text{-BuO})_2\text{SiO}]_3\text{H}$, which represent examples of the aforementioned alkoxysilanols **I**, **III**, and **IV** ($n = 2$, 3) respectively. These compounds are characterized by ^{29}Si NMR and IR spectroscopy and ESI MS in solution, and by ^{29}Si MAS NMR spectroscopy and X-ray crystallography in the solid state. Also described is the stepwise thermolysis of the most sensitive compound in this series, $(t\text{-BuO})_2\text{Si(OH)}_2$, to give amorphous silica.

RESULTS AND DISCUSSION

Synthetic aspects

The reaction of silicon tetrachloride, $SiCl_4$, with the appropriate amount of potassium *tert*-butoxylate, *t*-BuOK, provided tris(*tert*-butoxy)chlorosilane, $(t\text{-BuO})_3\text{SiCl}$ (**1**), and bis(*tert*-butoxy)dichlorosilane, $(t\text{-BuO})_2\text{SiCl}_2$ (**2**) in good yields (Eqn. (1)):

$$\text{SiCl}_4 + n\,t\text{-BuOK} \xrightarrow[-n\text{KCl}]{} \underset{\begin{matrix}\mathbf{1}\ (n=3)\\ \mathbf{2}\ (n=2)\end{matrix}}{(t\text{-BuO})_n\text{SiCl}_{4-n}} \qquad (1)$$

Both compounds were prepared previously by using *tert*-butanol and potassium or pyridine; however, these methods require the tedious drying of *tert*-butanol and/or removal of voluminous pyridinium chloride. We found the use of commercially available solid *t*-BuOK more convenient, particularly for small-scale reactions. Similarly, the reaction between hexachlorodisiloxane, $(Cl_3Si)_2O$, and four equivalents of *t*-BuOK afforded 1,1,3,3-tetrakis(*tert*-butoxy)-1,3-dichloro-1,3-disiloxane, $[(t\text{-BuO})_2\text{SiCl}]_2\text{O}$ (**3**), in good yields (Eqn. (2)):

$$(\text{Cl}_3\text{Si})_2\text{O} + 4t\text{-BuOK} \xrightarrow[-4\text{KCl}]{} \underset{\mathbf{3}}{[(t\text{-BuO})_2\text{SiCl}]_2\text{O}} \qquad (2)$$

The *tert*-butoxychlorosilanes **1**–**3** comprise colourless distillable oils, which were characterized by NMR spectroscopy and elemental analyses (Experimental section). The hydrolytic sensitivity of the chlorosilanes increases in the order $\mathbf{1} < \mathbf{3} \ll \mathbf{2}$.

The hydrolysis of **1**, **2**, and **3** with a large excess of water in the presence of a small excess of pyridine produced the corresponding silanols $(t\text{-BuO})_3\text{SiOH}$ (**4**), $(t\text{-BuO})_2\text{Si(OH)}_2$ (**5**), and $\text{HO}[(t\text{-BuO})_2\text{SiO}]_2\text{H}$ (**6**) in almost quantitative yields

(Eqns (3) and (4)):

$$\underset{\mathbf{1}\ (n=3)\ \mathbf{2}\ (n=2)}{(t\text{-BuO})_n\text{SiCl}_{4-n}} \xrightarrow[-\text{C}_5\text{H}_5\text{N}\cdot\text{HCl}]{\text{H}_2\text{O},\ \text{C}_5\text{H}_5\text{N}} \underset{\mathbf{4}\ (n=3)\ \mathbf{5}\ (n=2)}{(t\text{-BuO})_n\text{Si(OH)}_{4-n}} \quad (3)$$

$$\underset{\mathbf{3}}{[(t\text{-BuO})_2\text{SiCl}]_2\text{O}} \xrightarrow[-\text{C}_5\text{H}_5\text{N}\cdot\text{HCl}]{\text{H}_2\text{O},\ \text{C}_5\text{H}_5\text{N}} \underset{\mathbf{6}}{\text{HO}[(t\text{-BuO})_2\text{SiO}]_2\text{H}} \quad (4)$$

In order to achieve isolation of high yields of $(t\text{-BuO})_2\text{Si(OH)}_2$ (**5**), cooling below 10 °C is required during the reaction and work-up procedures, and the product isolated immediately. Apparently, higher temperatures and traces of pyridine in the mother liquor accelerate self-condensation to give resinous ill-defined materials.[24,27] No attempts were made to characterize these resinous materials. For a greater reproducibility, systematic studies were conducted on the thermolysis of pure $(t\text{-BuO})_2\text{Si(OH)}_2$ (**5**); these are reported below. *tert*-Butoxysilanols $(t\text{-BuO})_3\text{SiOH}$ (**4**) and $\text{HO}[(t\text{-BuO})_2\text{SiO}]_2\text{H}$ (**6**) show no or little tendency to undergo self-condensation in the presence of pyridine.

Tris(*tert*-butoxy)silanol, $(t\text{-BuO})_3\text{SiOH}$ (**4**), was previously prepared by hydrolyzing $(t\text{-BuO})_3\text{SiONa}$,[23] $(t\text{-BuO})_3\text{SiSH}$ in the presence of Ag_2O,[30] and $(t\text{-BuO})_3\text{SiCl}$ (**1**) with pyridine[28] or NH_4HCO_3.[32] The earlier synthesis of bis(*tert*-butoxy)silanediol, $(t\text{-BuO})_2\text{Si(OH)}_2$ (**5**), was by hydrolysis of $(t\text{-BuO})_2\text{Si(NH}_2)_2$[24] and $(t\text{-BuO})_2\text{SiCl}_2$ (**2**) with pyridine[27] or aniline[29] respectively. 1,1,3,3-Tetrakis(*tert*-butoxy)-1,3-siloxane-1,3-diol, $\text{HO}[(t\text{-BuO})_2\text{SiO}]_2\text{H}$ (**6**), has also been isolated previously in very poor yields by the hydrolysis of $(t\text{-BuO})_2\text{SiCl}_2$ (**2**) with pyridine.[27] The reaction conditions chosen in this work largely avoid less congenial by-products; the pyridinium chloride formed is dissolved in the water layer and thus can be removed easily.

The reaction of $(t\text{-BuO})_2\text{SiCl}_2$ (**2**) with two equivalents of $(t\text{-BuO})_2\text{Si(OH)}_2$ (**5**) in the presence of pyridine gave 1,1,3,3,5,5-hexakis(*tert*-butoxy)-1,3,5-trisiloxane-1,5-diol, $\text{HO}[(t\text{-BuO})_2\text{SiO}]_3\text{H}$ (**7**) in good yields along with a small amount of a resinous material that was not characterized (Eqn. (5)):

$$\underset{\mathbf{2}}{2(t\text{-BuO})_2\text{Si(OH)}_2} + \underset{\mathbf{5}}{(t\text{-BuO})_2\text{SiCl}_2} \xrightarrow[-2\text{C}_5\text{H}_5\text{N}\cdot\text{HCl}]{2\text{C}_5\text{H}_5\text{N}} \underset{\mathbf{7}}{\text{HO}[(t\text{-BuO})_2\text{SiO}]_3\text{H}} \quad (5)$$

Notably, there is no evidence that fully condensed *cyclo*-siloxanes, such as $[(t\text{-BuO})_2\text{SiO}]_3$,[53] were formed under these conditions. Although all of the *tert*-butoxysilanols **4–7** were prepared in previous studies, they were not fully characterized.

Crystal and molecular structures

The molecular structure of $(t\text{-BuO})_3\text{SiOH}$ (**4**) is shown in Fig. 1,[54] and selected geometric parameters are collected in the caption to the figure. Details of the structure determination are given in Table 1. The silicon atom exists in a distorted tetrahedral geometry defined by four oxygen atoms. The range of tetrahedral angles is quite narrow, being 105.28(9) to 114.9(1)°, with the narrowest angle subtended by the O(2) and O(4) atoms. The Si—O distances fall in two groups, with the shorter distances lying in the narrow range of 160.5(2) to 161.9(2) pm and the longest distance involving the O(2) atom (163.5(2) pm). Molecules that are related by a twofold axis of symmetry associate via hydrogen bonding interactions, and this provides an explanation for (i) the narrow O(2)—Si—O(4) angle and (ii) the longer Si—O(2) bond distance. In terms of the intermolecular association, the O(4)—H···O(2)^i separation is 183 pm, O(4)···O(2)^i is 280.8(3) pm, and the angle subtended at the hydrogen atom is 173° (symmetry operation i: $-x$, y, $1/2 - z$). Thus, the hydrogen-bonded framework features an eight-membered

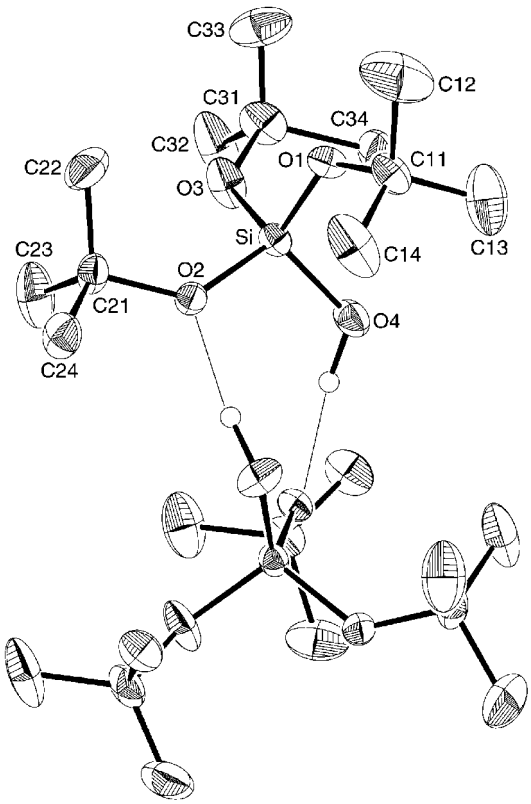

Figure 1. A symmetry (twofold) related pair of molecules of $(t\text{-BuO})_3\text{SiOH}$ (**4**) showing the crystallographic numbering scheme and mode of association between them; only one conformation of the disordered C(31)–C(34) *tert*-butyl group is shown and all carbon-bound hydrogen atoms have been omitted for clarity. Selected bond lengths (pm) and angles (°): Si—O(1) 161.9(2), Si—O(2) 163.5(2), Si—O(3) 160.5(2), Si—O(4) 161.0(2), O(1)—Si—O(2) 113.71(9), O(1)—Si—O(3) 107.2(1), O(1)—Si—O(4) 108.9(1), O(2)—Si—O(3) 107.0(1), O(2)—Si—O(4) 105.28(9), O(3)—Si—O(4) 114.9(1).

Table 1. Crystallographic parameters for $(t\text{-BuO})_3SiOH$ (**4**) and $HO[(t\text{-BuO})_2SiO]_2H$ (**6**)

	4	**6**
Mol. formula	$C_{12}H_{28}O_4Si$	$C_{16}H_{38}O_7Si_2$
Crystal size (mm^3)	$0.13 \times 0.24 \times 0.29$	$0.16 \times 0.24 \times 0.40$
Crystal system	Monoclinic	Triclinic
Space group	$C2/c$	$P\bar{1}$
Mol. weight	264.4	398.6
a (pm)	1684(1)	944.0(3)
b (pm)	957.4(4)	1103.4(2)
c (pm)	2113.4(7)	603.1(2)
α (deg)	90	92.97(2)
β (deg)	101.00(3)	98.57(3)
γ (deg)	90	112.91(2)
V ($Å^3$)	3337(2)	568.0(3)
Z	8	1
T (K)	173	173
D_{calc} ($g\,cm^{-3}$)	1.053	1.165
$F(000)$	1168	218
μ (mm^{-1})	0.143	0.186
No. of reflections collected	4203	5816
No. of unique reflections	3838	2613
No. of observed reflections $[I \geq 2\sigma(I)]$	2059	1648
GOF	1.03	1.00
Parameters	182	116
$wR_2(F^2)$ (all data)	0.157	0.144
R_1 (observed data)	0.048	0.051
Largest diff. peak (e^- $Å^{-3}$)	0.42	0.46

[···OSiOH···OSiOH] ring, similar to that found in the analogue $(RO)_3SiOH$ (RO = (1*S*)-*endo*-(−)-bornoxy).[35]

The molecular structure of $(t\text{-BuO})_3SiOH$ (**4**) is consistent with the observed solid-state NMR parameters. The ^{29}Si MAS NMR spectrum shows a single resonance at −88.8 ppm, whereas the ^{13}C MAS NMR spectrum reveals signals at 74.4, 73.6 and 73.0 ppm, which are assigned to three inequivalent tertiary carbon atoms of *tert*-butoxy groups. Consequently, three *tert*-butoxy groups in **4** are both magnetically and crystallographically inequivalent.

The molecular structure of $HO[(t\text{-BuO})_2SiO]_2H$ (**6**) is illustrated in Fig. 2,[54] and selected geometric parameters are collected in the caption to the figure.

The structure is centrosymmetric, with the O(3) atom constrained to lie on a crystallographic centre of inversion in the centrosymmetric space group $P\bar{1}$. The Si—O(3) distance is shorter, at 159.9(1) pm, than the other Si—O distances, but this may be an artefact of the data. It has been noted previously[55–61] that short Si—O bond distances, *i.e.* less than 162 pm, may be found in similar centrosymmetric structures; thus a careful analysis of the data is required, in particular the thermal displacement ellipsoids, as the observed linear arrangement may be simply an average of a disordered, non-linear arrangement. As artificial shortening of the Si—O(3) bond may arise in the present analysis, an analysis of the rigid body motion[62] was conducted on the silicon coordination geometry. While the expected elongations in the Si—O bond distances of up to 15 pm were noted, there was only a 6 pm increase in the Si—O(3) bond distance. The structure was also refined assuming no molecular symmetry, *i.e.* in the non-centrosymmetric $P1$ space group. This model resulted in an almost linear geometry at the O(3) atom, *i.e.* 178(1)°, and two distinct Si—O(3) distances of 157(1) and 162(1) pm, lending support to the centrosymmetric model. Accordingly, the following discussion will relate to the data obtained for the centrosymmetric model. The distortions from the ideal tetrahedral geometry in **6** are minimal, with the range of tetrahedral angles being 107.8(1) to 111.31(9)°. Aggregation between molecules is facilitated by hydrogen bonding interactions. Centrosymmetrically related molecules associ-

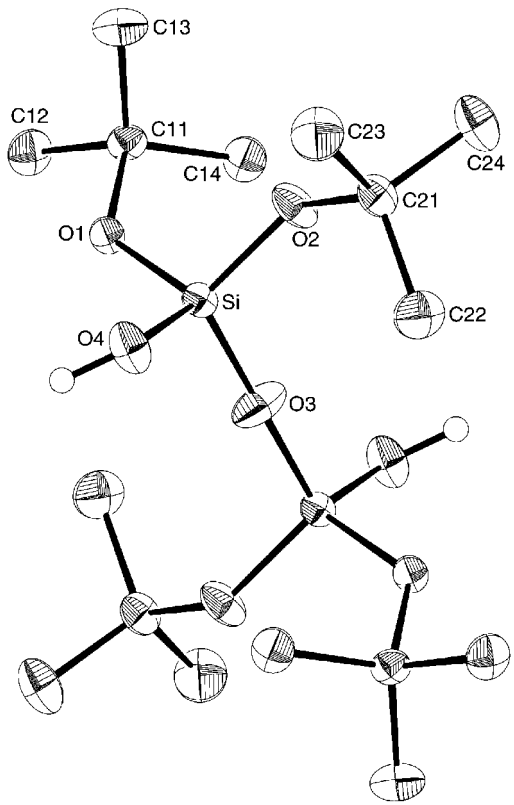

Figure 2. The molecular structure of centrosymmetric $HO[(t\text{-BuO})_2SiO]_2H$ (**6**) showing the crystallographic numbering scheme; only one conformation for each of the disordered methyl groups is shown and all carbon-bound hydrogen atoms have been omitted for clarity. Selected bond lengths (pm) and angles (°): Si—O(1) 163.0(2), Si—O(2) 160.0(2), Si—O(3) 159.25(8), Si—O(4) 160.4(2), O(1)—Si—O(2) 107.8(1), O(1)—Si—O(3) 108.47(7), O(1)—Si—O(4) 108.43(9), O(2)—Si—O(3) 111.31(9), O(2)—Si—O(4) 110.2(1), O(3)—Si—O(4) 110.55(8).

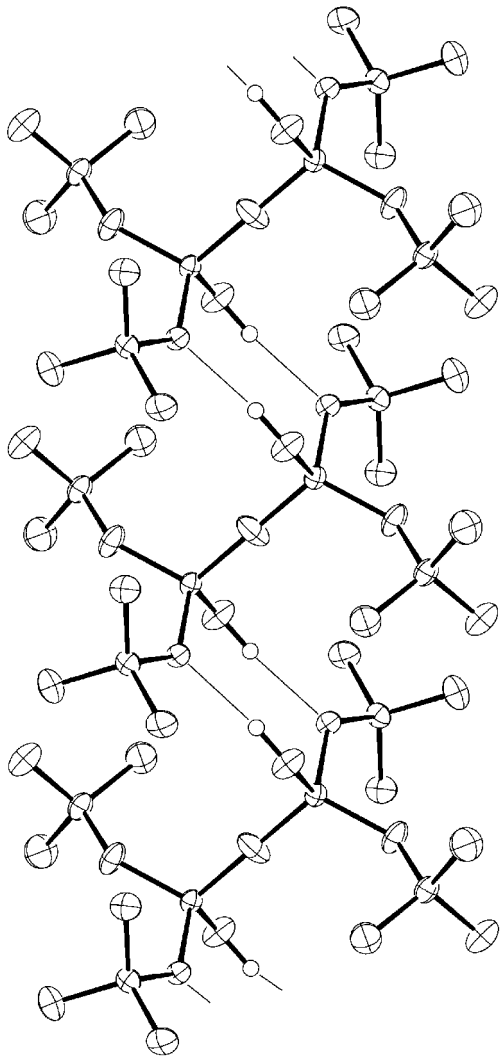

Figure 3. Chains of HO[(*t*-BuO)$_2$SiO]$_2$H (**6**) mediated by hydrogen-bonding interactions in the solid-state.

ate in the crystal structure so that O(4)—H is 192 pm from O(1)^i with O(4)···O(1)^i being 277.9(3) pm and the angle subtended at H being 174° (symmetry operation *i*: $-x$, $-y$, $-z$). As two hydrogen bonding interactions are formed by each molecule, a previously unreported chain structure incorporating [···OSiOH···OSiOH] rings results, as represented in Fig. 3.

The participation of the O(1) atom in the intermolecular interactions thus described accounts for its longer Si—O bond distance compared with the others. The centrosymmetric model is further supported by ^{29}Si MAS NMR spectroscopy, which shows only one signal centred at −95.1 ppm. Consistent with this, the ^{13}C MAS NMR spectrum exhibits two signals at 75.2 and 74.2 ppm, which are assigned to the tertiary carbon atoms of two magnetically inequivalent *tert*-butoxy groups.

The modes of association found in the crystal structures of

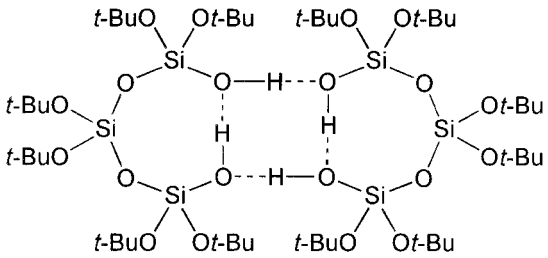

Figure 4. Molecular connectivity in **7**.

4 and **6** may hold some relevance for the mechanism of the alcohol-forming condensation of alkoxysilanols under sol–gel conditions. According to recent theoretical work,[63–65] silanols form hydrogen-bonded complexes, such as dimers containing eight-membered [···OSiOH···OSiOH] rings prior to condensation, in which the alkoxy or hydroxy groups are more reactive than in their non-associated parent compounds.[63–65] The crystal structure of (*t*-BuO)$_3$SiOH (**4**) resembles an example of such an activated complex. Given the established relation between the Si—O bond length and the Si—O bond strength,[66] the elongation of the Si—O bonds found for the *tert*-butoxy groups involved in the hydrogen bonding might be interpreted as Si—O bond activation.

Owing to the poor crystal quality only preliminary structural data were obtained for HO[(*t*-BuO)$_2$SiO]$_3$H (**7**), for which brief details of structural characteristics are described. The X-ray structure of **7*** reveals the expected molecular connectivity as represented in Fig. 4, and features a curved arrangement of the O—Si—O—Si—O—Si—O backbone of the molecule that undergoes cyclization owing to the presence of intramolecular hydrogen bonds formed between the two hydroxyl groups. Each ring thus formed is connected to a symmetry related (twofold) eight-membered ring via a second pair of hydrogen bonding interactions involving the two hydroxyl protons not involved in the formation of the original rings. This association mode results in the formation of hydrogen bonded 16-membered rings similar to that found for HO(Ph$_2$SiO)$_3$H,[67] but rather different to that found for (HOSi*t*-Bu$_2$O)$_2$SiMe$_2$.[68]

Obviously, this mode of association is favoured over alternative modes involving *tert*-butoxy groups. In view of the proposed condensation mechanism, the preference of this mode of association may also suggest why six-membered *cyclo*-trisiloxanes, [(RO)$_2$SiO]$_3$,[18] are kinetically formed during the sol–gel process, despite the fact that these species possess a considerable amount of ring strain.[69]

*Mol. formula: $C_{24}H_{56}O_{10}Si_3$; crystal system: monoclinic; space group: *C*2/*c*, mol. wt: 589.0; *a* (pm) 3009(2), *b* (pm) 1005.5(18), *c* (pm) 2517.2(17), β (deg) 108.86(4), *V* (nm^3) 7214(15), *Z* 8; *T* (K) 173; D_{calc} (d cm^{-3}) 1.085; *F*(000) 2576; μ (mm^{-1}) 0.174; no. of reflections collected: 8423; no. of unique reflections: 8268; no. of observed reflections [$I \geq 2\sigma(I)$]: 2990; $wR_2(F^2)$ (all data): 0.401; R_1 (observed data): 0.106.

Table 2. ^{29}Si NMR chemical shifts for *tert*-butoxysilanols **4**–**7**, $[(t\text{-BuO})_3\text{Si}]_2\text{O}$,[57] and $[(t\text{-BuO})_3\text{SiOSi(OH)}_2]_2\text{O}$[34] in solution and in the solid state

	$CDCl_3$	MeOD-d_3	DMSO-d_6	MAS
$(t\text{-BuO})_3\text{SiOH}$ (**4**)	−90.4[a]	−87.4[a]	−86.1[a]	−88.8
$(t\text{-BuO})_2\text{Si(OH)}_2$ (**5**)	−81.0[b]	−80.4[a]	−79.3[a]	−86.7
$\text{HO}[(t\text{-BuO})_2\text{SiO}]_2\text{H}$ (**6**)	−94.1[a]	−91.8[a]	−91.2[a]	−95.1
$\text{HO}[(t\text{-BuO})_2\text{SiO}]_3\text{H}$ (**7**)	−93.5, −104.4 (2:1)[a]	−91.8, −103.4 (2:1)[a]	−91.1, −102.8 (2:1)[a]	−96.0, −97.6, −108.2
$[(t\text{-BuO})_3\text{Si}]_2\text{O}$	−103.6[c,d]			
$[(t\text{-BuO})_3\text{SiOSi(OH)}_2]_2\text{O}$	−90.3, −103.2 (1:1)[c]			

[a] Conc. 0.5 g ml^{-1}.
[b] Conc. 0.2 g ml^{-1}.
[c] No concentration reported.
[d] No solvent reported.

^{29}Si NMR spectroscopy

The ^{29}Si NMR chemical shifts of the *tert*-butoxysilanols **4**–**7**, $[(t\text{-BuO})_3\text{Si}]_2\text{O}$,[57] and $[(t\text{-BuO})_3\text{SiOSi(OH)}_2]_2\text{O}$[34] in $CDCl_3$, MeOD–d_3, and DMSO–d_6 as well as in the solid-state are collected in Table 2. A first examination of the data shows that the ^{29}Si chemical shifts of *tert*-butoxysilanols **4**–**7** follow very similar trends reflecting the degree and strength of hydrogen bonding within the solvents. Thus, successive low-frequency shifts were observed by going from weakly polar $CDCl_3$, via MeOD–d_3, to strongly polar DMSO–d_6.[70] This observation correlates well with the fact that the condensation of alkoxysilanols occurs more rapidly in a non-polar solvent than in a polar solvent.[71,72] In view of the aforementioned condensation mechanism, a reasonable explanation for the lower hydrolysis rates may be the competitive blockage of the silanol groups by polar solvent molecules, thus preventing the formation of silanol dimers containing activated alkoxy or hydroxy groups.[63,64] This explanation is supported by the ^{29}Si MAS NMR chemical shifts of **5**–**7**, which are high-frequency shifted with respect to their ^{29}Si NMR chemical shifts in $CDCl_3$. The ^{29}Si MAS NMR chemical shift of **4**, however, lies between the ^{29}Si NMR chemical shifts measured in $CDCl_3$ and MeOD–d_3.

The collection of ^{29}Si NMR chemical shifts in MeOD–d_3 for the *tert*-butoxysilanols **4**–**7** and $[(t\text{-BuO})_3\text{Si}]_2\text{O}$ (no solvent reported)[57] also allows verification of the assignments made for sol–gel intermediates in previous works and comparison of the influence of the alkoxy groups, as well as of the different substitutions patterns.[6–21] Thus, comparison of tris(alkoxy)silanols $(t\text{-BuO})_3\text{SiOH}$ (**4**), $(\text{EtO})_3\text{SiOH}$, and $(\text{MeO})_3\text{SiOH}$ reveals that the ^{29}Si NMR chemical shifts increase steadily by going from *tert*-butyl to methyl groups (−87.4 ppm, −79.0 ppm, and −76.3 ppm respectively).[18] The same trend, albeit weaker, can be seen for the bis(alkoxy) silanediols $(t\text{-BuO})_2\text{Si(OH)}_2$ (**5**), $(\text{EtO})_2\text{Si(OH)}_2$, and $(\text{MeO})_2\text{Si(OH)}_2$, which show ^{29}Si NMR chemical shifts at −80.4 ppm, −76.5 ppm, and −74.8 ppm respectively.[18] The observed correlation between the ^{29}Si NMR chemical shifts and the organic groups agrees well with the results published for the systematic series of tetraalkoxysilanes, $(\text{RO})_4\text{Si}$,[73] and might be attributed to changes in the inductive effect rather than to the steric demand of the organic groups. The alkoxysiloxanes $[(\text{RO})_3\text{Si}]_2\text{O}$ and $\text{HO}[(\text{RO})_2\text{SiO}]_2\text{H}$ can be regarded as formal condensation products of the alkoxysilanols $(\text{RO})_3\text{SiOH}$ and $(\text{RO})_2\text{Si(OH)}_2$ respectively. For the *tert*-butoxysilanols the formal condensation from $(t\text{-BuO})_3\text{SiOH}$ (**4**) into $[(t\text{-BuO})_3\text{Si}]_2\text{O}$ and from $(t\text{-BuO})_2\text{Si(OH)}_2$ (**5**) into $\text{HO}[(t\text{-BuO})_2\text{SiO}]_2\text{H}$ (**6**) coincides with a change in the ^{29}Si NMR chemical shifts of 16.2 ppm (−87.4 to −103.6 ppm) and 11.4 ppm (−80.4 to −91.8 ppm) respectively. Consistently, the formal condensation of $(\text{MeO})_3\text{SiOH}$ into $[(\text{MeO})_3\text{Si}]_2\text{O}$ and of $(\text{MeO})_2\text{Si(OH)}_2$ into $\text{HO}[(\text{MeO})_2\text{SiO}]_2\text{H}$ gives rise to changes in the ^{29}Si NMR resonances of 9.7 ppm (−76.3 to −86.0 ppm) and 9.4 ppm (−74.8 to −84.2 ppm) respectively.[18]

It is important to note that, in principle, the concentration of silanols is another parameter that may also influence the ^{29}Si chemical shifts. However, when avoiding extreme concentration differences, this effect lies within the experimental error of the measured ^{29}Si chemical shifts.[74]

IR spectroscopy

The IR absorptions (KBr disks) for the *tert*-butoxysilanols **4**–**7** between 4000 and 400 cm^{-1} are listed in Table 3. Owing to the great similarity of the IR spectra and the high number of IR absorptions ascribed to the *tert*-butoxy groups, only tentative assignments of the vibrational modes were made by consulting the abundant IR data available from the literature.[75–80] A normal coordinate analysis appeared not to be justified. The most notable features in the IR spectra appear in the OH stretching vibrations, which divide the *tert*-butoxysilanols **4**–**7** into two groups, namely $(t\text{-BuO})_3\text{SiOH}$ (**4**) and $\text{HO}[(t\text{-BuO})_2\text{SiO}]_2\text{H}$ (**6**), which show absorptions at 3398 cm^{-1} and 3406 cm^{-1} respectively, and $(t\text{-BuO})_2\text{Si(OH)}_2$ (**5**) and $\text{HO}[(t\text{-BuO})_2\text{SiO}]_2\text{H}$ (**7**), which reveal absorptions at 3333 cm^{-1} and 3356 cm^{-1} respectively. In view of the established molecular structures, these differences are attributed to the different hydrogen bonding modes.

Table 3. IR absorptions (KBr) for *tert*-butoxysilanols **4**–**7** and the material **P1** between 4000 and 400 cm^{-1} and tentative assignments

4	5	6	7	P1	Assignment[a]
3398 s, br	3333 s, br	3406 s, br	3356 s, br	3449 s, br	ν(OH)
2976 vs	2979 vs	2979 vs	2977.7 vs	2979 vs	$\nu_{sym}(CH_3)$
2932 w	2932 w	2932 w	2931 w	2934 w	
2908 sh	2912 sh	2908 sh	2909 sh	2911 sh	$\nu_{asym}(CH_3)$
2874 w	2871 w	2874 w	2877 w	2876 w	
1475 m	1474 m	1472 m	1474 m	1474 m	$\delta_{asym}(CH_3)$
1458 sh	1460 sh	1458 sh	1459 sh	1458 sh	
1393 m	1391 m	1393 m	1391 m	1393 m	$\delta_{sym}(CH_3)$
1367 s	1367 s	1369 s	1366 s	1369 s	
1242 m		1244 m	1244 m	1248 m	$\rho(CCH_3) + \nu$(CC)
1192 s	1193 s	1196 s	1194 s	1195 s	$\rho(CCH_3) + \nu$(CO)
1054 vs	1072 vs	1065 s	1058 vs		ν_{asym}(SiOX)(X = C, Si)
		1045 s			
1010 s	1027 s	1015 s	1027 s	1016 vs, br	ν(CC)
907 s	892 s	903 s	889 s	901 s	δ(SiOH)
	871 sh				ν(CC)
826 vs	820 vs	825 vs	834 vs	821 vs	ν(CC)
		802 vs	804 vs		
788 m	791 m	787 m	787 m	790 m	ν(CC)
	757 sh	756 sh			
	745 m	738 m	741 m	743 m	
700 s	702 s	702 s	703 s	702 s	
	640 m	644 m	647 m	668 m	
627 m			623 m	621 m	
562 w	563 w	562 w	565 w	564 w	δ(OSiO)
514 m	517 m	529 m	513 m	512 m	ν_{sym}(SiOC)
483 s	481 s	483 s	489 s	485 s	δ_{asym}(SiOC)
428 w	433 w	431 w	430 w	437 w	

[a] Abbreviations: v = very, s = strong, m = medium, w = weak, sh = shoulder, br = broad; ν = stretching, δ = deformation, ρ = rocking, sym = symmetric, asym = asymmetric.

Additionally, IR absorptions found slightly above and below 900 cm^{-1} are assigned to SiOH deformation vibrations, reflecting the aforementioned differences: (t-BuO)$_3$SiOH (**4**) and HO[(t-BuO)$_2$SiO]$_2$H (**6**) exhibit absorptions at 907 cm^{-1} and 903 cm^{-1} respectively, whereas (t-BuO)$_2$Si(OH)$_2$ (**5**) and HO[(t-BuO)$_2$SiO]$_3$H (**7**) absorb at 892/871 cm^{-1} and 889 cm^{-1} respectively. Moreover, the IR spectra of **4**–**7** show intense bands around 1050 cm^{-1}, which are assigned to asymmetric SiOC and SiOSi stretching vibrations; however, in all relevant cases, the latter was always obscured by the former, thereby precluding a reliable assessment of the presence of siloxane linkages. Notably, the absorption bands afforded by the *tert*-butoxy groups only change marginally, due to the insulating effect of the oxygen atoms.[77]

Additionally, IR spectra of the *tert*-butoxysilanols **4**–**7** were also recorded in chloroform solution (conc. 10%) to investigate the degree of association. In all cases two signals were observed in the range between 3800 and 3100 cm^{-1}, which were unambiguously assigned to OH stretching vibrations of free and associated silanol groups;[81,82] at 3680 and 3391 cm^{-1} for (t-BuO)$_3$SiOH (**4**), 3668 and 3406 cm^{-1} for (t-BuO)$_2$Si(OH)$_2$ (**5**), 3678 and 3441 cm^{-1} for HO[(t-BuO)$_2$SiO]$_2$H (**6**), and 3678 and 3487 cm^{-1} for HO[(t-BuO)$_2$SiO]$_3$H (**7**). This assignment is supported by the shape and intensity of the signals. The signals related to the free silanol groups are sharp and have low intensity, whereas the signals of the associated silanol groups are broader and have higher intensity. Thus, the presence of free and associated silanol groups is in agreement with an equilibrium between alkoxysilanol monomers and hydrogen-bonded complexes taking place in chloroform.

ESI MS

To identify ionic species being related with the parent *tert*-butoxysilanols in acetronitrile, ESI MS spectra (cone voltage: 40 V) of **4**–**7** were recorded in both positive and negative modes. The following mass clusters showing the expected isotopic pattern were found: (t-BuO)$_3$SiOH (**4**), positive

mode: $[\mathbf{4}+\mathrm{Na}]^+$ (287.2), $[2\times\mathbf{4}+\mathrm{Na}]^+$ (551.3); negative mode: $[\mathbf{4}-\mathrm{H}]^-$ (263.2), $[2\times\mathbf{4}-\mathrm{H}]^-$ (527.3); $(t\text{-BuO})_2\mathrm{Si(OH)}_2$ (**5**), positive mode: $[\mathbf{5}+\mathrm{Na}+\mathrm{MeCN}]^+$ (272.1), $[2\times\mathbf{5}+\mathrm{Na}]^+$ (439.2); negative mode: $[\mathbf{5}+\mathrm{Cl}]^-$ (243.1); $\mathrm{HO[(}t\text{-BuO)}_2\mathrm{SiO]}_2\mathrm{H}$ (**6**), positive mode: $[\mathbf{6}+\mathrm{Na}]^+$ (421.2), $[2\times\mathbf{6}+\mathrm{Na}]^+$ (819.4); negative mode: $[2\times\mathbf{6}+\mathrm{Cl}]^-$ (433.2); $\mathrm{HO[(}t\text{-BuO)}_2\mathrm{SiO]}_3\mathrm{H}$ (**7**), positive mode: $[\mathbf{7}+\mathrm{Na}]^+$ (611.3), $[2\times\mathbf{7}+\mathrm{Na}]^+$ (1199.6); negative mode: $[\mathbf{7}-\mathrm{H}]^-$ (587.3), $[\mathbf{7}+\mathrm{Cl}]^-$ (623.3).

In the positive mode, the most remarkable observation is not the readily formed 1:1 and 2:1 adducts of the *tert*-butoxysilanols **4–7** with sodium cations, but the complete lack of protonated silanols under these conditions. It is noteworthy that preferential adduct formation of alkoxysilanols with sodium cations has also been reported for labile intermediates of the sol–gel process.[83] The observation of 2:1 adducts is consistent with the presence of hydrogen-bonded aggregates of the *tert*-butoxysilanols **4–7** in solution. In the negative mode the observed mass clusters are in agreement with the deprotonated *tert*-butoxysilanols (for **4** and **7**) and 1:1 and 2:1 adducts of the *tert*-butoxysilanols with chloride anions (for **5–7**).

For the detection of protonated silanols, the authentic samples of **4–7** were acidified with 1 M hydrochloric acid (10 µl ml^{-1} sample solution) and immediately measured again in the positive mode (cone voltage: optimized for each sample between 10 and 120 V). In all cases, mass clusters corresponding to the protonated *tert*-butoxysilanols **4–7** were observed, though with somewhat low intensity: $(t\text{-BuO})_3\mathrm{SiOH}$ (**4**), positive mode: $[\mathbf{4}+\mathrm{H}]^+$ (265.2), $[2\times\mathbf{4}+\mathrm{H}]^+$ (529.4); $(t\text{-BuO})_2\mathrm{Si(OH)}_2$ (**5**), positive mode: $[\mathbf{5}+\mathrm{H}]^+$ (209.1); $\mathrm{HO[(}t\text{-BuO)}_2\mathrm{SiO]}_2\mathrm{H}$ (**6**), positive mode: $[\mathbf{6}+\mathrm{H}]^+$ (399.2); $\mathrm{HO[}t\text{-BuO)}_2\mathrm{SiO]}_3\mathrm{H}$ (**7**), positive mode: $[\mathbf{7}+\mathrm{H}]^+$ (589.3).

Thermolysis of $(t\text{-BuO})_2\mathrm{Si(OH)}_2$ (5)

In order to investigate systematically the resinous materials obtained from the self-condensation of $(t\text{-BuO})_2\mathrm{Si(OH)}_2$ (**5**), a pure sample of **5** was heated under reflux for 24 h in a small quantity of hexane (in the absence of a catalyst). The use of hexane was necessary to render a homogeneous reaction mixture. After the removal of solvent a resinous material was obtained, which, according to ^{29}Si NMR spectroscopy (CDCl_3), still contained substantial amounts of unreacted $(t\text{-BuO})_2\mathrm{Si(OH)}_2$ (**5**) ($\delta-81.1$) and a smaller amount of $\mathrm{HO[(}t\text{-BuO)}_2\mathrm{SiO]}_2\mathrm{H}$ (**6**) ($\delta-93.8$). The presence of higher oligomers and polymers was also apparent, from the presence of some very broad signals between −92.5 and −102.3 ppm. However, the broadness of the signals in combination with the poor signal-to-noise ratio precluded further interpretation regarding the nature of these species.

To achieve further condensation, the resinous material was heated without solvent for 48 h at 100 °C. On cooling, a colourless transparent glass-like material formed, hereafter referred to as **P1**. The material **P1** appears insoluble in common organic solvents, although it swells. X-ray powder diffraction confirmed the amorphous nature of the material **P1**. Elemental analysis of the material **P1** revealed that the carbon and hydrogen content decreased with respect to its precursor, $(t\text{-BuO})_2\mathrm{Si(OH)}_2\mathrm{Si(OH)}_2$ (**5**), from 46.12% and 9.68% to 37.81% and 8.25% respectively, which suggests that both water and alcohol-forming condensation has occurred. The IR spectrum (KBr disks) of **P1** resembles that of the molecular *tert*-butoxysilanols **4–7** (Table 3). A very broad and intense absorption at 3448.9 cm^{-1} confirms the presence of hydroxy groups in material **P1**. The nature of the material **P1** was further studied by ^{29}Si MAS NMR spectroscopy. Whereas $(t\text{-BuO})_2\mathrm{Si(OH)}_2$ (**5**) shows a sharp signal at −86.7 ppm (Fig. 5a), material **P1** exhibits a broad signal with maxima at −94.5 and −104.5 ppm and shoulders at −97.3 and −110.2 ppm (Figure 5b). The signals at −94.5 ppm and −104.5 ppm are tentatively assigned to silicon sites having $(t\text{-BuO})_2\mathrm{Si(OH)(OSi)}$ and $(t\text{-BuO})\mathrm{Si}_2\mathrm{(OSi)}_2$ environments respectively. The ^{13}C MAS NMR spectrum of material **P1** shows two somewhat broad signals at 73.0 ppm and 31.0 ppm that were assigned to the tertiary and primary carbon atoms respectively of the *tert*-butoxy groups. No evidence was found for encapsulated *tert*-butanol or any other organic by-products.

Material **P1** shows no melting point; however, at temperatures exceeding 180 °C the particles shrink in size and a colourless liquid condenses at the top of the melting tube, thus indicating that condensation takes place. This observation is consistent with a thermogravimetric analysis (TGA) of

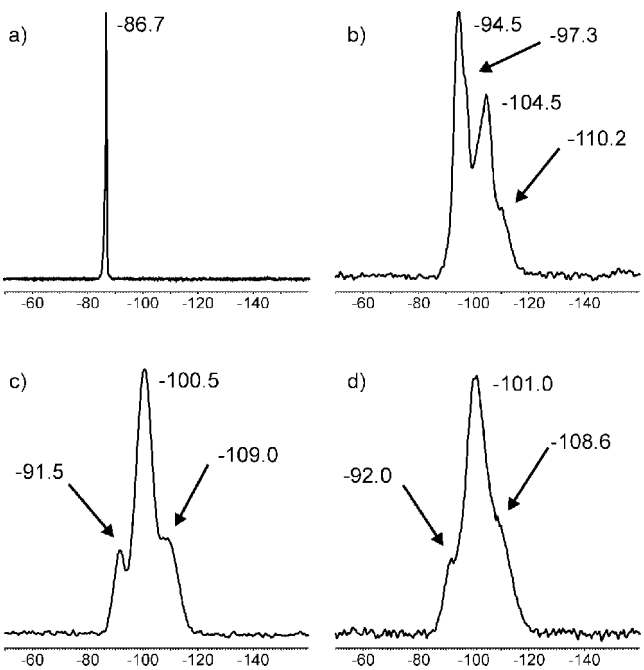

Figure 5. ^{29}Si MAS NMR spectra (79.42 MHz) of (a) $(t\text{-BuO})_2\mathrm{Si(OH)}_2$ (**5**), and the thermolysis products (b) **P1**, (c) **P2**, and (d) **P3** (chemical shifts in ppm).

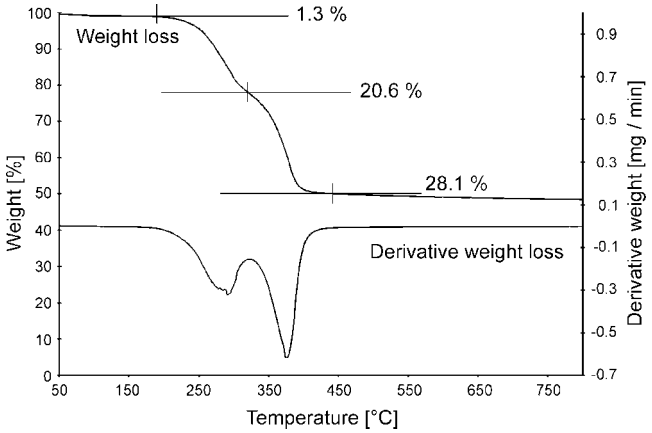

Figure 6. TGA trace for the material **P1** under air (10 °C min^{-1}).

material **P1** (Fig. 6). Thus, between 50 and 200 °C only a small weight loss (1.3%) occurred. The first substantial weight loss (20.6%) took place between 200 and 320 °C, with a maximum at 280 °C. A second major weight loss (28.1%) occurred between 320 and 450 °C, with a maximum at 380 °C. Then, in the range between 450 and 850 °C, again only a small mass loss (1.6%) was observed.

Taking into account the two major weight loss incidents under TGA conditions, a bulk sample of material **P1** was thermolysed at 320 °C for 1 h in an attempt to obtain an incompletely decomposed intermediate that still contained an appreciable amount of carbon. However, the observed weight loss of approximately 55% indicated the cleavage of almost all organic matter. No attempts were made to identify the volatile organic by-products of the bulk thermolysis. However, in previous work these compounds were identified as being mainly *tert*-butanol, isobutene, and water.[28] The residue of the thermolysis at 320 °C was a glass-like slightly brownish material, hereafter referred to as **P2**, for which residual carbon and hydrogen contents of 0.40% and 2.14% respectively were found. This suggests that **P2** consists of impure silica, $[SiO_{n/2}(OH)_{4-n}]_m$. This is supported by a featureless IR spectrum (KBr), which resembles that published for pure silica.[79] Conclusive evidence was provided by the ^{29}Si MAS NMR spectrum of **P2**, which reveals a broad signal with a maximum at −100.5 ppm and two shoulders at −91.5 and −109.0 ppm that are unambiguously assigned to the well-established Q_2, Q_3, and Q_4 sites in hydrated silica (Fig. 5c).[84]

Further heating of material **P2** at 800 °C for 4 h eventually afforded a glass-like pale yellowish material, hereafter referred to as **P3**, for which residual carbon and hydrogen contents of 0.29% and 1.17% respectively were found. Consistent with material **P2**, the ^{29}Si MAS NMR spectrum of **P3** showed a broad signal with a maximum at −101.0 ppm and two shoulders at −92.0 and −108.6 ppm (Fig. 5d). Featureless X-ray powder diffraction spectra confirm that materials **P2** and **P3** are amorphous.

EXPERIMENTAL

General remarks

All operations with sensitive compounds were carried out under argon using standard vacuum line and Schlenk techniques. All solvents were dried over the appropriate desiccants and distilled prior to use. $SiCl_4$, $(Cl_3Si)_2O$, and *t*-BuOK were commercial products. Solution NMR spectra were obtained using a Varian 300 MHz Unity Plus NMR spectrometer. ^{1}H, ^{13}C, and ^{29}Si chemical shifts are given in ppm and are referenced against Me_4Si. Solid-state NMR spectra were measured using a JEOL Eclipse Plus 400 MHz NMR spectrometer. Adamantane (δ 38.6/29.5) and $(Me_3Si)_4Si$ (δ − 9.9/−135.6) were used as secondary references against Me_4Si. IR spectra were recorded using a TTS 3000 MX BioRad FTIR spectrophotometer as KBr disks or as 10% solution in chloroform between NaCl plates. Electrospray mass spectra were obtained with a Platform II single quadrupole mass spectrometer (Micromass, Altrincham, UK) using an acetonitrile mobile phase. Acetonitrile solutions (0.1 mM) of the compounds were injected directly into the spectrometer via a Rheodyne injector equipped with a 50 µl loop. A Harvard 22 syringe pump delivered the solutions to the vaporization nozzle of the electrospray ion source at a flow rate of 10 µl min^{-1}. Nitrogen was used as both a drying gas and for nebulization with flow rates of approximately 200 ml min^{-1} and 20 ml min^{-1} respectively. Pressure in the mass analyser region was usually about 4×10^{-5} mbar. Typically, ten signal-averaged spectra were collected. The TGA was made on a Perkin–Elmer TGA 7 thermogravimetric analyser (with TAC 7/DX controller and gas selector). Microanalyses were performed by CMAS, Belmont, Australia.

Synthesis of $(t\text{-BuO})_3SiCl$ (1), $(t\text{-BuO})_2SiCl_2$ (2), and $[(t\text{-BuO})_2SiCl]_2O$ (3)

To a solution of $SiCl_4$ (34.0 g, 200 mmol for **1**; 51.0 g, 300 mmol for **2**) or $(Cl_3Si)_2O$ (42.7 g, 150 mmol for **3**) in hexane (300 ml) were added small portions of solid *t*-BuOK (67.3 g, 600 mmol) within 1 h at 0 °C. The mixture was stirred for 2 h at room temperature before being heated at reflux for 10 h. The precipitate was filtered, and the hexane was removed by condensation. The crude product was purified by vacuum distillation.

(t-BuO)$_3$SiCl (**1**): yield 48.7 g, 172 mmol, 86%; b.p. 65 °C/400 Pa. ^{1}H NMR ($CDCl_3$) δ: 1.35 (s, 27H; *t*-Bu). ^{13}C NMR ($CDCl_3$) δ: 74.9 (CMe_3), 31.1 (CMe_3). ^{29}Si NMR (neat/D_2O cap.) δ: −85.6. Anal. Found: C, 50.70; H, 9.65. Calc. for $C_{12}H_{27}ClO_3Si$ (282.88): C, 50.95; H, 9.62%.

(t-BuO)$_2$SiCl$_2$ (**2**): yield 60.3 g, 246 mmol, 82%; b.p. 50 °C/400 Pa. ^{1}H NMR ($CDCl_3$) δ: 1.42 (s, 18H; *t*-Bu). ^{13}C NMR ($CDCl_3$) δ: 77.8 (CMe_3), 31.0 (CMe_3). ^{29}Si NMR (neat/D_2O cap.) δ: −70.0. Anal. Found: C, 39.50; H, 7.35. Calc. for $C_8H_{18}Cl_2O_2Si$ (245.22): C, 39.18; H, 7.40%.

[(t-BuO)$_2$SiCl]$_2$O (**3**): yield 51.0 g, 117 mmol, 78%; b.p.

95 °C/400 Pa. ^{1}H NMR ($CDCl_3$) δ: 1.38 (s, 36H; *t*-Bu). ^{13}C NMR ($CDCl_3$) δ: 75.5 (CMe_3), 31.1 (CMe_3). ^{29}Si NMR (neat/D_2O cap.) δ: −89.5. Anal. Found: C, 44.35; H, 8.50. Calc. for $C_{16}H_{36}Cl_2O_5Si_2$ (435.54): C, 44.12; H, 8.33%.

Synthesis of (*t*-BuO)$_3$SiOH (4), (*t*-BuO)$_2$Si(OH)$_2$ (5), and HO[(*t*-BuO)$_2$SiO]$_2$H (6)

A solution of the *tert*-butoxychlorosilane (**1**, 28.2 g, 100 mmol for **4**; **2**, 12.3 g, 50 mmol for **5**; **3**, 21.8 g, 50 mmol for **6**) and pyridine (9.1 g, 115 mmol) in dry ether (100 ml) was slowly added to a mixture of water (250 ml) and ether (250 ml) at 0 °C. For **4**, the mixture was heated under reflux for 24 h; for **5** and **6**, the mixture stirred for 30 min at 0 °C. The layers were immediately separated, the organic layer washed with ice water (2 × 50 ml) and dried over Na_2SO_4. The volatile components were removed under reduced pressure at room temperature (for **4** and **6**) or 0 °C (for **5**). The solid or semi-solid residues were immediately recrystallized from hexane (for **4** and **6**) or chloroform (for **5**).

(*t*-BuO)$_3$SiOH (**4**), 24.3 g, 92 mmol (92%), m.p. 65–66 °C (lit. 62–63 °C,[30] 65–66 °C,[28] 65.5–66 °C,[23] 63–65 °C[32]). ^{1}H NMR ($CDCl_3$) δ: 1.32 (s, 27H; *t*-Bu). ^{13}C NMR ($CDCl_3$) δ: 73.0 (CMe_3), 31.2 (CMe_3). ^{13}C MAS NMR δ: 74.4, 73.6, 73.0 (CMe_3), 32.9, 32.5, 32.0 (CMe_3). Anal. Found: C, 54.05; H, 10.80. Calc. for $C_{12}H_{28}O_4Si$ (264.44): C, 54.51; H, 10.67%.

(*t*-BuO)$_2$Si(OH)$_2$ (**5**), 9.0 g, 43 mmol (86%), m.p. 107 °C (lit. 99–101 °C,[24] 101–102 °C,[29] 101–103 °C[27]). ^{1}H NMR ($CDCl_3$) δ: 1.35 (s, 18H; *t*-Bu). ^{13}C NMR ($CDCl_3$) δ: 73.4 (CMe_3), 31.2 (CMe_3). ^{13}C MAS NMR δ: 73.9, 73.3, 73.0 (CMe_3), 32.8, 32.6, 32.3 (CMe_3). Anal. Found: C, 46.33; H, 9.57. Calc. for $C_8H_{20}O_4Si$ (208.33): C, 46.12; H, 9.68%.

HO[(*t*-BuO)$_2$SiO]$_2$H (**6**), 17.1 g, 43 mmol (85%), m.p. 82 °C (lit. 77 °C[27]). ^{1}H NMR ($CDCl_3$) δ: 1.30 (s, 36H; *t*-Bu). ^{13}C NMR ($CDCl_3$) δ: 73.3 (CMe_3), 32.2 (CMe_3). ^{13}C MAS NMR δ: 75.2, 74.2 (CMe_3), 32.6, 31.7 (CMe_3). Anal. Found: C, 48.17; H, 9.77. Calc. for $C_{16}H_{38}O_7Si_2$ (398.65): C, 48.21; H, 9.61%.

Synthesis of HO[(*t*-BuO)$_2$SiO]$_3$H (7)

To a solution of **5** (4.17 g, 20.0 mmol) in toluene (30 ml), pyridine (3.96 g, 50.0 mmol) and then, slowly, **2** (2.34 g, 10.0 mmol) were added via a syringe at 0 °C. Immediately, a colourless precipitation was formed. The mixture was stirred for 30 min at room temperature and then heated for 4 h at 80 °C. After cooling to room temperature, the mixture was filtered and the filtrate hydrolysed with water (20 ml). The layers were separated, the organic layer dried over Na_2SO_4, and the volatiles removed under reduced pressure at room temperature. The semi-solid residue was recrystallized from hexane at −10 °C to give colourless crystals of **7** (2.79 g, 4.73 mmol (47%), m.p. 71 °C (lit. 61–63 °C[27])). ^{1}H NMR ($CDCl_3$) δ: 1.31 (s, 36H; *t*-Bu). ^{13}C NMR ($CDCl_3$) δ: 73.3 (CMe_3), 73.2 (CMe_3), 32.2 (CMe_3). ^{13}C MAS NMR δ: 73.5, 73.4, 73.2, 73.0 (CMe_3), 32.8, 32.4, 32.0, 31.7 (CMe_3). Anal. Found: C, 49.10; H, 9.55. Calc. for $C_{24}H_{56}O_{10}Si_3$ (588.96): C, 48.94; H, 9.58%.

Thermolysis of (*t*-BuO)$_2$Si(OH)$_2$ (5)

A sample of **5** (4.16 g, 20.0 mmol) was dissolved in hexane (20 ml) and heated under reflux for 24 h. Removal of the solvent in vacuum afforded a resinous material. This material was heated without solvent for 48 h at 100 °C. On cooling, a colourless transparent material, **P1**, was obtained. **P1** was heated for 1 h at 320 °C and provided a slightly brownish residue, **P2**. Further heating of **P2** for 4 h at 800 °C produced a pale yellowish material, **P3**. The characterization is described in the text.

X-ray crystallographic study

Data collections were performed at 173 K on a Rigaku AFC7R diffractometer fitted with Mo Kα radiation employing the ω–2θ scan technique so that θ_{max} was 27.5°. Data were processed with teXsan,[62] solved with DIRDIF[85] and refined on F^2 using SHELXL97.[86] Disorder in the C32–C34 methyl atoms was modelled in **4** so that each atom was assigned two positions of equal weight (from refinement). The O—H atoms were located from the respective difference maps and included in the model without refinement. The diagrams were drawn with ORTEP using 30% probability ellipsoids.[54]

Crystallographic data (excluding structure factors) for the structures reported in this paper have been deposited with the Cambridge Crystallographic Data Centre as supplementary publication no. CCDC-150975 (**4**) and CCDC-165213 (**6**). Copies of the data can be obtained free of charge on application to CCDC, 12 Union Road, Cambridge CB2 1EZ, UK [fax: +44(1223)336-033; e-mail: deposit@ccdc.cam.ac.uk].

Acknowledgements

The Australian Research Council is thanked for financial support. We are indebted to Dr François Ribot (CNRS/Pierre and Marie Curie University, Paris, France) for critically reviewing this work. Peter Laming (RMIT University, Melbourne, Australia) is gratefully acknowledged for the TGA.

REFERENCES

1. Hench LL and West JK. *Chem. Rev.* 1990; **90**: 33.
2. Brinker C and Scherer G (eds). *Sol–Gel Science: The Physics and Chemistry of Sol–Gel Processing*. Academic Press: 1990.
3. Hench LL (ed.). *Sol–Gel Silica: Properties, Processing and Technology Transfer*. Noyes Publications: 1998.
4. Mackenzie JD. *J. Non-Cryst. Solids* 1988; **100**: 162.
5. Brinker CJ. *J. Non-Cryst. Solids* 1988; **100**: 31.
6. Pouxviel JC, Boilot JP, Beloeil JC and Lallemand JY. *J. Non-Cryst. Solids* 1987; **89**: 345.
7. Pouxviel JC and Boilot JP. *J. Non-Cryst. Solids* 1987; **94**: 374.
8. Assink RA and Kay BD. *J. Non-Cryst. Solids* 1988; **99**: 359.
9. Assink R and Kay BD. *J. Non-Cryst. Solids* 1988; **107**: 35.
10. Kelts LW and Armstrong NJ. *J. Mater. Res.* 1989; **4**: 423.
11. Chojnowski J, Cypryk M, Kazmierski K and Rozga K. *J. Non-Cryst. Solids* 1990; **125**: 40.
12. Boonstra AH and Baken JME. *J. Non-Cryst. Solids* 1990; **122**: 171.
13. Damrau U and Marsmann HC. *J. Non-Cryst. Solids* 1991; **135**: 15.
14. Assink RA and Kay BD. *Annu. Rev. Mater. Sci.* 1991; **21**: 491.

15. Sanchez J and McCormick A. *J. Phys. Chem.* 1992; **96**: 8973.
16. Bernards TNM, Oomen EWJL, Van Bommel MJ and Boonstra AH. *J. Non-Cryst. Solids* 1992; **142**: 215.
17. Brunet F, Lux P and Virlet J. *New J. Chem.* 1994; **18**: 1059.
18. Damrau U and Marsmann HC. *J. Non-Cryst. Solids* 1994; **168**: 42.
19. Alam TM, Assink RA, Prabakar S and Douglas AL. *Magn. Reson. Chem.* 1996; **34**: 603.
20. Mazur M, Mlynarik V, Valko M and Pelikan P. *Appl. Magn. Reson.* 1999; **16**: 547.
21. Mazur M, Mlynarik V, Valko M and Pelikan P. *Appl. Magn. Reson.* 2000; **18**: 187.
22. Bernards TNM, Van Bommel MJ and Boonstra AH. *J. Non-Cryst. Solids* 1991; **134**: 1.
23. Backer HJ and Klasens HA. *Rec. Trav. Chim.* 1942; **61**: 500.
24. Miner CS, Bryan LA, Holysz RP and Pedlow GW. *Ind. Eng. Chem.* 1947; **39**: 1368.
25. Morgan CR, Olds WF and Rafferty AL. *J. Am. Chem. Soc.* 1951; **73**: 5193.
26. Wright JR, Bolt RO, Goldschmidt A and Abbott AD. *J. Am. Chem. Soc.* 1958; **80**: 1733.
27. Schott G and Kibbel HU. *Z. Anorg. Allg. Chem.* 1961; **311**: 53.
28. Abe Y and Kijima I. *Bull. Chem. Soc. Jpn.* 1969; **42**: 1118.
29. Abe Y and Kijima I. *Bull. Chem. Soc. Jpn.* 1970; **43**: 466.
30. Wojnowski W. *Z. Anorg. Allg. Chem.* 1974; **403**: 186.
31. Schott G and Engelbrecht L. *Z. Chem.* 1978; **18**: 457.
32. Schott G, Engelbrecht L and Holdt HJ. *Z. Anorg. Allg. Chem.* 1979; **459**: 177.
33. Holdt HJ, Schott G, Popowski E and Kelling H. *Z. Chem.* 1983; **23**: 252.
34. Rulkens R, Coles MP and Tilley TD. *Dalton Trans.* 2000; 627.
35. Beckmann J, Dakternieks D and Tiekink ERT. *J. Organomet. Chem.* 2002; **648**: 188.
36. Kijima I, Yamamoto T and Abe Y. *Bull. Chem. Soc. Jpn.* 1971; **44**: 3193.
37. Abe Y, Hayama K and Kijima I. *Bull. Chem. Soc. Jpn.* 1972; **45**: 1258.
38. Terry KW, Ganzel PK and Tilley TD. *Chem. Mater.* 1992; **4**: 1290.
39. Gunji T, Kasahara T, Fujii A, Abe Y and Kawano M. *Bull. Chem. Soc. Jpn.* 1995; **68**: 2975.
40. Gunji T, Kitakatsu T and Abe Y. *Bull. Chem. Soc. Jpn.* 1995; **68**: 2951.
41. Terry KW, Lugmair CG and Tilley TD. *J. Am. Chem. Soc.* 1997; **119**: 9745.
42. Rulkens R and Tilley TD. *J. Am. Chem. Soc.* 1998; **120**: 9959.
43. Rulkens R, Male JL, Terry KW, Olthof B, Khodakov A, Bell AT, Iglesia E and Tilley TD. *Chem. Mater.* 1999; **11**: 2966.
44. Coles MP, Lugmair CG, Terry KW and Tilley TD. *Chem. Mater.* 2000; **12**: 122.
45. Fujdala KL and Tilley TD. *Chem. Mater.* 2001; **13**: 1817.
46. Murugavel R, Voigt A, Walawalkar MG and Roesky HW. *Chem. Rev.* 1996; **96**: 2205.
47. King L and Sullivan AC. *Coord. Chem. Rev.* 1999; **189**: 19.
48. Lorenz V, Fischer A, Giessmann S, Gilje JW, Gun'ko Y, Jacob K and Edelmann FT. *Coord. Chem. Rev.* 2000; **206–207**: 321.
49. Beckmann J and Jurkschat K. *Coord. Chem. Rev.* 2001; **215**: 267.
50. Markiewicz WT and Adrych K. *Nucleosides Nucleotides* 1988; **7**: 671.
51. Markiewicz WT, Nowakowska B and Adrych K. *Tetrahedron Lett.* 1988; **29**: 1561.
52. Markiewicz WT and Adrych-Rozek K. *Nucleosides Nucleotides* 1991; **10**: 415.
53. Basenko SV and Voronkov MG. *Russ. J. Gen. Chem.* 1997; **67**: 1029.
54. Johnson CK. *ORTEP*. Report ORNL-5138, Oak Ridge National Laboratory, TN, USA, 1976.
55. Glidewell C and Liles DC. *Acta Crystallogr. Sect. B* 1978; **34**: 124.
56. Glidewell C and Liles DC. *J. Organomet. Chem.* 1981; **212**: 291.
57. Wojnowski W, Bochenska W, Peters K, Peters EM and Von Schnering HG. *Z. Anorg. Allg. Chem.* 1986; **533**: 165.
58. Shklover VE, Bürgi HB, Raselli A, Armbruster T and Hummel W. *Acta Crystallogr. Sect. B* 1991; **47**: 544.
59. He J, Harrod JF and Hynes R. *Organometallics* 1994; **13**: 2496.
60. Rudert R and Schmaucks G. *Acta Crystallogr. Sect. C* 1994; **50**: 631.
61. Bürgi HB. *Acta Crystallogr. Sect. B* 1995; **51**: 571.
62. *teXsan, Single Crystal Structure Analysis Software*, Version 1.04. Molecular Structure Corporation, The Woodlands, TX, USA, 1997.
63. Kudo T and Gordon MS. *J. Am. Chem. Soc.* 1998; **120**: 11 432.
64. Okumoto S, Fujita N and Yamabe S. *J. Phys. Chem. A* 1998; **102**: 3991.
65. Kudo T and Gordon MS. *J. Phys. Chem. A* 2000; **104**: 4058.
66. Brown ID and Shannon RD. *Acta Crystallogr. Sect. A* 1973; **29**: 266.
67. Behbehani H, Brisdon BJ, Mahon MF, Molloy KC and Mazhar M. *J. Organomet. Chem.* 1993; **463**: 41.
68. Graalmann O, Klingebiel U, Clegg W, Haase M and Sheldrick GM. *Chem. Ber.* 1984; **117**: 2988.
69. Haiduc I. *The Chemistry of Inorganic Ring Systems, Pt. 1*. Wiley–Interscience: 1970.
70. Williams EA, Cargioli JD and Larochelle RW. *J. Organomet. Chem.* 1976; **108**: 153.
71. Artaki I, Zerda TW and Jonas J. *Mater. Lett.* 1985; **3**: 493.
72. Artaki I, Zerda TW and Jonas J. *J. Non-Cryst. Solids* 1986; **81**: 381.
73. Curran MD, Gedris TE and Stiegman AE. *Chem. Mater.* 1998; **10**: 1604.
74. Kretschmer A and Backer M. *J. Organomet. Chem.* 2001; **628**: 233.
75. Okawara R. *Bull. Chem. Soc. Jpn.* 1958; **31**: 154.
76. Smith AL and McHard JA. *Anal. Chem.* 1959; **31**: 1174.
77. Ory HA. *Anal. Chem.* 1960; **32**: 509.
78. Smith AL. *Spectrochim. Acta* 1960; **16**: 87.
79. Smith AL. *Spectrochim. Acta* 1963; **19**: 849.
80. Kriegsmann H. *Pure Appl. Chem.* 1966; **13**: 203.
81. Harris GI. *J. Chem. Soc.* 1963; 5978.
82. Harris GI. *J. Chem. Soc. B* 1970; 488.
83. Bossio RE, Callahan SD, Stiegman AE and Marshall AG. *Chem. Mater.* 2001; **13**: 2097.
84. Engelhardt G and Koller H. *NMR – Basic Princ. Prog.* 1994; **31**: 1.
85. Beurskens PT, Admiraal G, Beurskens G, Bosman WP, García-Granda S, Smits JMM and Smykalla C. *The DIRDIF program system*. Technical Report of the Crystallography Laboratory, University of Nijmegen, The Netherlands, 1992.
86. Sheldrick GM. *SHELXL97*. University of Göttingen, Germany, 1997.

